



**HAL**  
open science

## **Influence of rainfall spatial variability on hydrological modelling: a simulation approach**

Isabelle Emmanuel, Hervé Andrieu, E Leblois, N Janey

► **To cite this version:**

Isabelle Emmanuel, Hervé Andrieu, E Leblois, N Janey. Influence of rainfall spatial variability on hydrological modelling: a simulation approach. Weather Radar and Hydrology, Apr 2014, France. 10p. hal-00966170

**HAL Id: hal-00966170**

**<https://hal.science/hal-00966170>**

Submitted on 26 Mar 2014

**HAL** is a multi-disciplinary open access archive for the deposit and dissemination of scientific research documents, whether they are published or not. The documents may come from teaching and research institutions in France or abroad, or from public or private research centers.

L'archive ouverte pluridisciplinaire **HAL**, est destinée au dépôt et à la diffusion de documents scientifiques de niveau recherche, publiés ou non, émanant des établissements d'enseignement et de recherche français ou étrangers, des laboratoires publics ou privés.

# Influence of rainfall spatial variability on hydrological modelling: a simulation approach

I. Emmanuel<sup>(1)</sup>, H. Andrieu<sup>(1)</sup>, E. Leblois<sup>(2)</sup> and N. Janey<sup>(3)</sup>

<sup>(1)</sup> PRES L'UNAM, IFSTTAR, Département GERS, and IRSTV, FR CNRS 248, Bouguenais, France

[isabelle.emmanuel@ifsttar.fr](mailto:isabelle.emmanuel@ifsttar.fr) ; Tel: 0033 1 81 66 80 81

<sup>(2)</sup> IRSTEA, Unité hydrologique-hydraulique, Lyon, France

<sup>(3)</sup> Université de Franche-Comté, Département Informatique, UFR ST, Besançon, France

## Abstract

The present work aims to quantify the effects of neglecting rainfall spatial variability for runoff modelling at the outlet of catchments of about ten to several hundred km<sup>2</sup>. In order to overcome modelling and rainfall data errors, to control the rainfall variability as well as characteristics and hydrological behavior of catchments, we have proceeded by simulation. For this, a simulation chain has been used, including a stream network model, a rainfall simulator and a distributed hydrological model (with four production functions and a distributed transfer). The choice has been made not to be exhaustive but to study very contrasted situations. Results showed that it is difficult to obtain robust general conclusions by studying only a few rainfall events which might explain that different conclusions were drawn in previous case studies. However, some tendencies were observed. For the different studied rainfall configurations, the effect of neglecting rainfall variability is particularly important if: 1) the dimensionless ratio “velocity of rainfall field on celerity along flow path” is small, 2) the rainfall field direction is perpendicular to the catchment flow direction, 3) the catchment has an elongated shape and 4) an Horton or SCS production function.

**Keywords:** Rainfall spatial variability, Hydrological modelling, Rainfall simulator, Stream network model

## INTRODUCTION

The link between rainfall space-time variability and hydrological modelling at a catchment outlet remains an open research issue in hydrology. It puts the following question: what is the effect of neglecting rainfall spatial variability in hydrological modelling? This question has been tackled by numerous studies and results are contrasted. For example, Adams *et al.* (2012) notice that routing averaging effects remove the majority of the impact of rainfall spatial variability at the catchment scale (150 km<sup>2</sup>). The analysis of a storm event occurred in Germany on the Weisseritz catchment (384 km<sup>2</sup>) led Tarolli *et al.* (2013) to the similar conclusion. However, Zoccatelli *et al.* (2010), who studied three extreme flash flood events on catchments of 36 km<sup>2</sup> to 167 km<sup>2</sup> in Romania, report that neglecting spatial rainfall variability results in a considerable loss of modelling efficiency in about 30% of the cases. The influence of the rainfall measurement error on runoff modelling can also be significant (Quintero *et al.*, 2012), and contributes to hide the gain of accuracy allowed by a detailed knowledge of the rainfall variability.

In this context, we suggest proceeding by simulation in order to evaluate for which catchments characteristics and for which rainfall types neglecting rainfall spatial variability has an effect on the hydrological modelling of catchments for which the surface runoff is the dominant process. Simulation enables us to explore a high number of situations in order to gain a general point of view. Moreover, it allows overcoming different sources of errors (rainfall and flows data, modelling) and controlling as much as possible rainfall variability and catchments characteristics (area, shape, hydrological behavior). In this way, we have developed a simulation chain composed of three independent modules: a stream network model, a rainfall simulator and a distributed hydrological model.

## PRESENTATION OF THE SIMULATION CHAIN

### Stream network model

The stream network model (Janey, 1992; Emmanuel, 2011) is based on the diffusion limited aggregation (DLA) method which builds tree networks from the random walk of particles on a

lattice. It allows the simulation of catchments of determined area with random irregular shape and different stream network organization. Emmanuel (2011) showed that the generated stream networks have morphometric properties similar to those of real networks. For a detailed presentation of the stream network model, the reader may refer to Emmanuel (2011).

### **Rainfall simulator**

The rainfall simulator, called SAMPO, acronym for Simulation of Advected Mesoscale Precipitations and their Occurrence (Leblois and Creutin, 2013), is based on the Turning Band Method which has been adapted to simulate time series of rainfall fields at chosen spatial and temporal resolutions. The final simulated rainfall field is obtained by the product of two independent fields: 1) an indicator field of zero and nonzero rainfall pixels defining the outline of the rainy areas; 2) a field of nonzero rainfall defining the inner rainfall variability. The displacement of the rainfall field is defined by the direction and the velocity of the advection. One main characteristic of SAMPO is that it simulates realistic temporal evolution of rainfall fields of given types. For a detailed presentation of SAMPO, the reader may refer to Leblois and Creutin (2013).

### **Hydrological model**

The catchment acts as a spatio-temporal filter which smooths the rainfall variability in time and space. The rainfall pattern is transformed on hillslopes into a net rainfall pattern which is aggregated and routed as flow in the stream network. In order to represent in a simple and robust way the most influential processes, the hydrological model is based on the following hypotheses: 1) the production function is applied at the catchment cell scale and reproduces the main types of runoff generation processes, 2) the surface runoff is the dominant process on hillslopes and the travel time on hillslopes is shorter than the travel time in the stream network, 3) the flow characteristics in the stream network are independent of net rainfall. According to these hypotheses, the production function gives a net rainfall pattern at the catchment cell (equivalent to a rainfall pixel) scale which is, in a second step, routed by the transfer function to the catchment outlet. Both functions are fully distributed at the catchment cell scale.

#### *Production function*

Rainfall variability influences particularly the fast response of catchments. Therefore, the hydrological model considers several production functions describing this fast response, supposed to correspond to surface runoff on hillslopes. The aim is to consider production functions which are widely used and for which rainfall variability acts in different ways allowing to obtain different patterns of net rainfall over the studied catchments. The following production functions have been considered to obtain different hydrological behavior:

- constant runoff coefficient (denoted CRC): a constant runoff coefficient (RC in %) is applied to all the catchment cells;
- a contributive area model (CA): the RC% cells of the catchment, displaying the highest topographic index, form the contributive areas. Those cells have a net rainfall of 100%;
- US Soil Conservation Service (SCS): the potential maximum retention ( $S_{SCS}$  in mm) is computed such that, at the event scale, RC% of the raw rainfall is transformed into net rainfall.
- a Horton model (H): the infiltration capacity ( $P_H$  in mm/h) is computed such that, at the event scale, RC% of the raw rainfall is transformed into net rainfall. For a given cell and time step, with a raw rainfall  $P$ , the net rainfall is equal to 0 if  $P < P_H$ , otherwise, its value is  $P - P_H$ .

#### *Transfer function*

In most flood routing applications, the Saint-Venant equations can be simplified and lead to the diffusive wave model. This model depends on two parameters: the celerity (C) and the diffusivity (D). Generally, these two parameters are function of the discharge. In the particular case where C

and  $D$  are assumed to be constant during the rainfall event and in the case of a semi-infinite channel, the diffusive wave model admits an analytical solution: the Hayami model which is a linear model (Moussa, 1996). For sake of simplicity, it is assumed that the flow velocities on hillslope and in the stream network are equal. As the hillslope travel time is assumed to be much less than the stream network travel time, this simplification weakly affects the total travel time. Therefore, net rainfall of each catchment cell  $u$  is routed to the outlet of the catchment using the Hayami kernel function (Moussa, 1996) defined as:

$$K_u(t) = \frac{L_u}{2(\pi D)^{1/2}} \frac{\exp\left[\frac{CL_u}{4D} \left(2 - \frac{L_u}{Ct} - \frac{Ct}{L_u}\right)\right]}{t^{3/2}} \quad (1)$$

with  $t$  the time,  $L$  the stream path length (in m) from the considered cell  $u$  to the catchment outlet,  $C$  the celerity (in m/s) and  $D$  the diffusivity (in  $\text{m}^2/\text{s}$ ).

The flow at the catchment outlet is given by the expression:

$$Q(t) = \frac{10^{-3}S}{3600} \sum_{u=1}^{u=n} P_n(u, t) * K_u(t) \quad (2)$$

with  $Q(t)$  the flow (in  $\text{m}^3/\text{s}$ ),  $S$  the cell area (in  $\text{m}^2$ ),  $t$  the time,  $n$  the number of cells belonging to the catchment,  $P_n(u, t)$  the net rainfall of the cell  $u$  (in  $\text{mm}/\text{h}$ ),  $K_u(t)$  the Kernel function of cell  $u$  (in  $\text{s}^{-1}$ ) defined in equation 1. \* represents the convolution product.

## PRESENTATION OF THE CASE STUDY

In this study, the presented simulation chain is used to evaluate for which catchments characteristics and for which rainfall types neglecting rainfall spatial variability has an effect on flow modelling at the catchment outlet. The proposed approach is original. We have made the choice to work on contrasting situations. For this purpose, we have simulated time series of rainfall fields with a temporal and a spatial variability more or less important. Those time series of rainfall fields are used to force catchments of different area, shape and hydrological behavior which are also simulated.

This section presents the characteristics of the simulated catchments and of their hydrological behavior as well as the characteristics of the rainfall events. The criteria used to evaluate the effect of ignoring rainfall spatial variability on flow hydrographs are discussed in the last part of this section.

### Characteristics of the simulated catchments and of their hydrological behavior

Four areas of 10  $\text{km}^2$ , 30  $\text{km}^2$ , 90  $\text{km}^2$  and 270  $\text{km}^2$  have been considered in order to cover the range of areas of urban or peri-urban catchments of fast hydrological response which depends highly on the rainfall input.

The stream network model can simulate catchments of random and irregular shapes (Emmanuel, 2011). However, in this study we have decided to work with given, regular and schematic shapes (Figure 1). The influence of working with regular and schematic shapes rather than with irregular and random shapes is discussed in the results section. Our objective being to consider contrasting shapes of different elongations, three shapes have been considered (Figure 1): an elongated shape, an oblate shape and a nearly circular shape (named hereafter the intermediate shape). Those three shapes have been defined so that their elongation coefficient is, respectively, less than 1 (equal to 0.6), higher than 1 (equal to 1.2), close to 1 (equal to 0.9). The elongation coefficient is equal to the ratio between the diameter of the circle having the same area as the catchment and the catchment maximum length (Schumm, 1956).

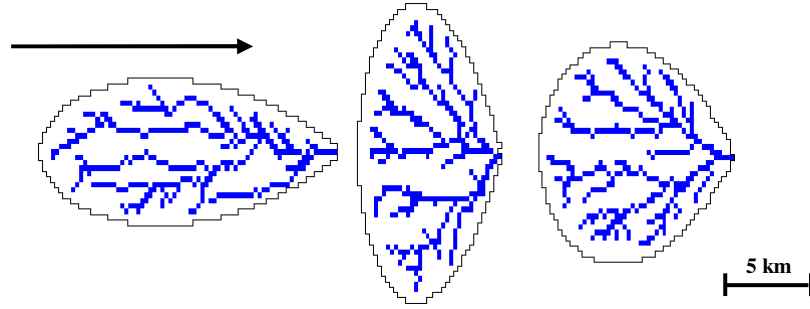


Figure 1: 90 km<sup>2</sup> simulated catchments with an elongated (left), oblate (middle) and intermediate shape (right). For the figure, the stream networks are represented with a drainage area threshold of 0.5 km<sup>2</sup>. The main flow direction is indicated by the arrow.

The four production functions have been constrained to restore the same event runoff coefficient ( $RC$ ), in order to obtain, for each simulated rainfall event, the same runoff volume and thus to make the results comparable. In this case study,  $RC$  has been taken equal to 0.3. The transfer being independent of the net rainfall value, the value of  $RC$  does not influence the transfer.

The studied catchments are divided in 250 m x 250 m cells (same areas as rainfall pixels, cf. following part) and represent hillslopes. Three values of celerity have been considered:  $C = 0.5$  m/s,  $C = 1$  m/s and  $C = 2$  m/s. As Moussa and Bocquillon (1996) indicate that the diffusive wave model is more sensitive to the parameter  $C$  than to  $D$ , a value of  $D = 500$  m<sup>2</sup>/s has been adopted. The values of  $C$  and  $D$  have been chosen in order to cover the range of response time of small catchments up to about 300 km<sup>2</sup> (cf. Table 1).

The following “reference” case has been defined: a catchment of 90 km<sup>2</sup> area, of intermediate shape with a SCS production function, with  $C = 1$  m/s. The values of area and  $C$  have been chosen to correspond to the intermediate value of each parameter range. The SCS production function has been chosen as it is widely used. In order to evaluate the sensitivity to a given parameter, only the values of this specific parameter (area, shape, production function, celerity) are to vary, while the three other parameters remain equal to the reference values.

A total of 11 catchments scenarios are obtained (called hereafter by the names contained in Table 1) which characteristics are summarized in Table 1.

Name	Fixed parameters				Obtained characteristics		
	Area (km <sup>2</sup> )	Shape	Production function	$C$ (m/s)	$L_{max}$ (km)	Response time (h)	Concentration time (h)
<b>Reference</b>	<b>90</b>	<b>Intermediate</b>	<b>SCS</b>	<b>1</b>	12.25	2h00	5h45
A10	10	<b>Intermediate</b>	<b>SCS</b>	<b>1</b>	3.75	0.5h	2h40
A30	30	<b>Intermediate</b>	<b>SCS</b>	<b>1</b>	7	1h00	3h50
A270	270	<b>Intermediate</b>	<b>SCS</b>	<b>1</b>	21.25	4h00	8h50
El	<b>90</b>	Elongated	<b>SCS</b>	<b>1</b>	18.25	3h25	7h45
Ob	<b>90</b>	Oblate	<b>SCS</b>	<b>1</b>	9	1h45	4h50
CRC	<b>90</b>	<b>Intermediate</b>	CRC	<b>1</b>	12.25	2h00	5h45
CA	<b>90</b>	<b>Intermediate</b>	CA	<b>1</b>	12.25	2h00	5h45
Horton	<b>90</b>	<b>Intermediate</b>	Horton	<b>1</b>	12.25	2h00	5h45
C05	<b>90</b>	<b>Intermediate</b>	<b>SCS</b>	0.5	12.25	3h25	12h00
C2	<b>90</b>	<b>Intermediate</b>	<b>SCS</b>	2	12.25	1h10	2h30

Table 1: Characteristics and name of the different considered catchments.  $L_{max}$  corresponds to the length of the longest hydrological path. Values relative to the reference catchment are in bold.

### Characteristics of the simulated rainfall events

SAMPO has been used to simulate rainfall events with a spatial resolution of 250 m x 250 m over a window of 30 km x 30 km (higher than the spatial extent of all considered catchments). In this

case study, a rainfall event corresponds to a time series of rainfall fields of 5 min temporal resolution and of 12h00 duration (corresponding to the highest concentration time of the different catchments, *cf.* Table 1). During the rainfall-runoff simulations, the catchments centers of gravity are located in the center of the simulation window.

Our goal being to consider contrasted rainfall types more or less variable, six rainfall types (RT1 to RT6) have been considered with RT1 less variable than RT2, which is less variable than RT3, etc. A simulated image of each rainfall field type is shown on Figure 2.

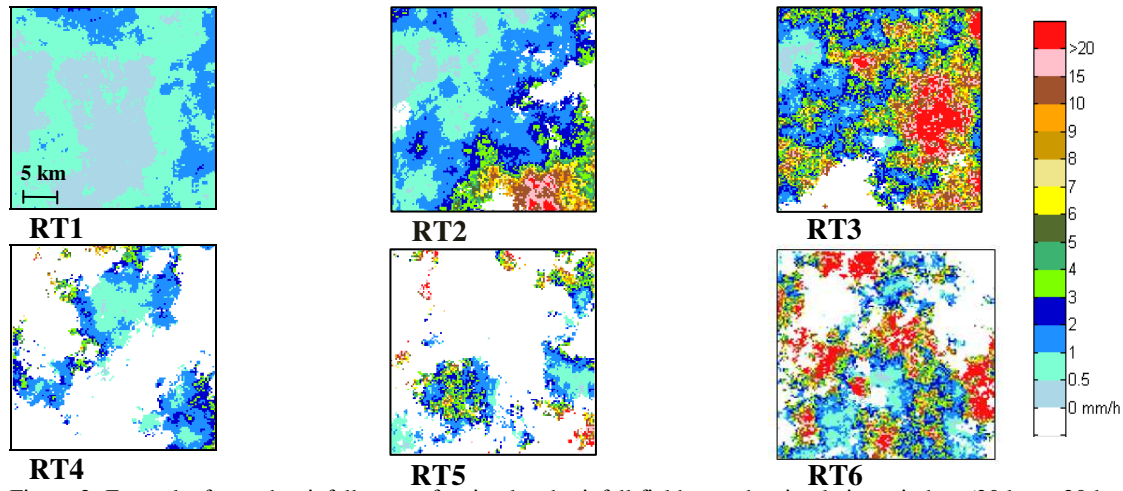


Figure 2: Example, for each rainfall type, of a simulated rainfall field over the simulation window (30 km x 30 km) at a temporal resolution of 5 min and at a spatial resolution of 250 m x 250 m.

The second objective is to consider time series of rainfall fields which last more or less over the catchment. For this, for each rainfall type, 3 advection velocities have been defined: 2.5 (denoted V2.5), 5 (V5) and 10 m/s (V10).

Finally, different rainfall fields' directions have been studied by considering three directions of advection: 1) from upstream to downstream, 2) from downstream to upstream and 3) perpendicular to the main flows direction of the catchment and downward, which is equivalent to the direction upward as the considered catchments are symmetrical.

Therefore, in this case study, 54 configurations of rainfall have been defined as well as 11 catchments scenarios that are used to evaluate the effect of neglecting rainfall spatial variability on flow modelling at the catchment outlet.

### Criteria used to evaluate the effect of neglecting rainfall spatial variability

The objective is to quantify the effect of neglecting rainfall spatial variability on rainfall-runoff hydrographs. Thus, two spatial rainfall resolutions have been considered: 1) the simulated rainfall spatial resolution (spatial resolution of 250 m x 250 m, called “distributed rainfall”), and 2) spatially uniform rainfall (called “average rainfall”) and their associated obtained hydrographs have been compared. Average rainfall is computed, at each time step, by averaging the distributed rainfall of each catchment cell. Thus, at each time step, each catchment cell receives the same amount of raw rainfall. Moreover, the total event raw rainfall over the catchment is the same both for the distributed and the average rainfall.

In order to obtain robust results, 50 rainfall events have been simulated for each of the 54 configurations of rainfall. Thus, for each of the 11 catchments scenarios and for each of the 54 configurations of rainfall, 50 pairs of hydrographs are obtained, each pair regrouping a “distributed hydrograph” obtained from the distributed rainfall and an “average hydrograph” obtained from the average rainfall. The distributed hydrographs are taken as reference. The differences between each pair of hydrographs (distributed and average) give an indication about the errors in runoff response

modelling arising by neglecting rainfall spatial variability. The differences between each pair of hydrographs are assessed by the relative absolute error (RAE):

$$RAE = \frac{|Q_{Dmax} - Q_{Amax}|}{Q_{Dmax}} * 100 \quad (3)$$

with  $Q_{Dmax}$  the maximum value of the distributed hydrograph and  $Q_{Amax}$  the maximum value on the average hydrograph. For each case, 50 values of RAE are obtained. The value that is presented is the quantile 80% (denoted  $RAE_{80}$  in %). The quantile  $RAE_{80}$  means that 20% of the studied values are higher than  $RAE_{80}$ . The highest are the values of  $RAE_{80}$ , the biggest are the differences between distributed and average hydrographs.

## RESULTS

In this paper, results of catchment shape and production functions are not presented but only given in the Conclusion.

### Influence of a given, schematic and regular catchment shape and of stream networks organization

The proposed methodology simulates the influence of rainfall variability on three schematic catchments of regular shapes with one stream network organization. This simplification allows us to limit the number of simulations. It is based on the assumption that all the catchments of a given area with the same elongation behave similarly regarding rainfall variability. The validity of the proposed methodology has been confirmed in two steps:

1) 10 catchments of 90 km<sup>2</sup> and of elongation coefficient equals to the one of the reference catchment (i.e. equals to 0.9) have been simulated (an example is given on Figure 3). Those 10 catchments have been submitted to the 50 rainfall events of each of the six rainfall types (with V5 and an upstream-downstream direction). The  $RAE_{80}$  have been computed on the obtained pairs of hydrographs. It appears that  $RAE_{80}$  computed for the irregular shape catchments are very close to those of the reference catchment (Figure 3). Therefore, the schematic and regular chosen shapes can be considered, in the framework of this study, as representative of irregular shapes of same elongation coefficient.

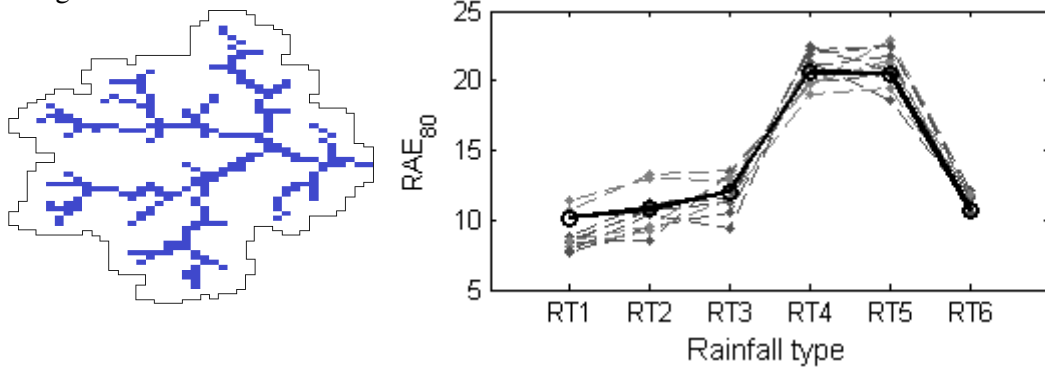


Figure 3: Example of a catchment of irregular shape of 90 km<sup>2</sup> and of elongation coefficient equals to 0.9. Evolution of  $RAE_{80}$  (in %), computed for the reference scenario, in function of the rainfall type for the catchment of schematic and regular shape (circle in bold) and for the 10 catchments of irregular shapes (points).

2) 100 reference catchments of different stream networks organization have been submitted to 50 events of RT3 type (with V5 and an upstream-downstream direction). The obtained  $RAE_{80}$  are very similar: they range between 11.4% and 12.8%. As the precise organization of the stream network has only a small influence in our study, we have considered only one stream network organization for each catchment scenario.

### General remarks on the RAE distributions

In addition to the  $RAE_{80}$ , the mean and the standard deviation associated to the RAE distribution have been computed for the 11 catchments scenarios with a rainfall type RT5, a velocity V2.5 and a perpendicular direction (Figure 4). This rainfall configuration engenders, for all catchments scenarios, the highest differences between distributed and average hydrographs.

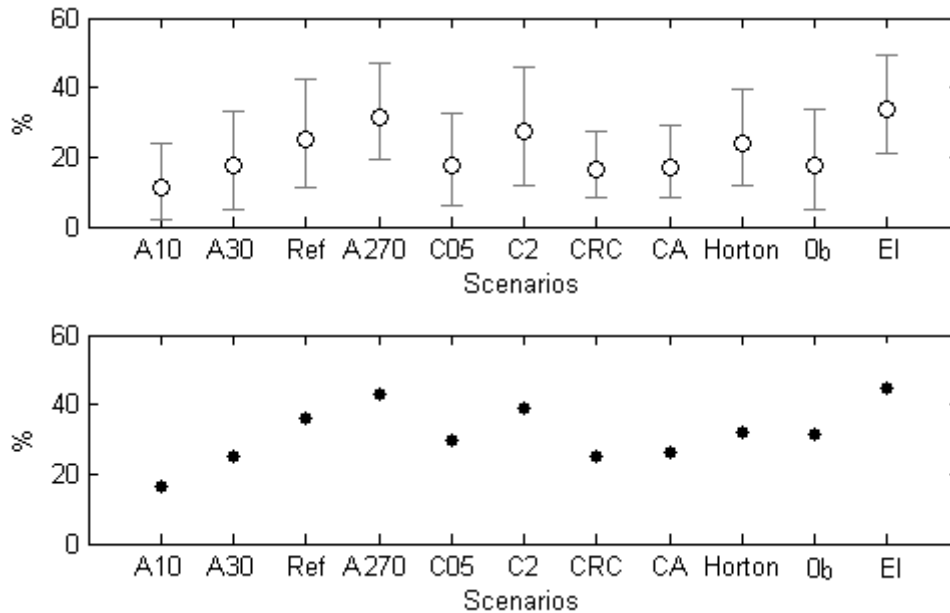


Figure 4: Evolution of the mean (circle) more or less the standard deviation (lines) (up). Evolution of  $RAE_{80}$  (points) (down). The statistical scores are computed for each catchment scenarios for RT5 with V2.5 and a perpendicular rainfall field direction.

Figure 4 gives, for each catchment scenario, an indication on the highest observed differences between distributed and average hydrographs. Those differences are the highest for the scenario EI (cf. Table 1), for which the mean of RAE equals 34% and  $RAE_{80}$  equals to 45%. This means that for the catchment with an elongated shape forced by a rainfall type RT5, moving at V2.5 in the perpendicular direction of the catchment, the maximum value of the 50 detailed hydrographs and the corresponding value on the average hydrographs differ with a mean of 34%. In addition, 20% of the studied pairs present an  $RAE$  higher than 45%.

Moreover, the computed standard deviations are high. The variation coefficients (ratio between the standard deviation and the average) range, in this example, between 100% for the scenario A10 and 43% for the scenario EI. These results show that there is a high dispersion of the RAE around their mean. The dispersion inside a scenario is higher than the dispersion between the different scenarios. This observation is verified for all the rainfall types' configurations. It clearly confirms that it is difficult to obtain reliable general conclusions, on the influence of neglecting rainfall spatial variability, from only the study of a few rainfall events. It also contributes to explain why the study of a limited number of events can reach to different conclusions.

### Influence of the rainfall type (spatial extent of the rainfall fields) evaluated on the reference catchment

The influence of the rainfall type is illustrated here, for the reference scenario, with V5 and an upstream-downstream direction. As the advection velocity is the same for all rainfall types, the evaluation of the influence of rainfall type is equivalent to the evaluation of the influence of the spatial extent of rainfall fields.

$RAE_{80}$  is close for RT1, RT2 and RT3 (equals to 10 – 12%) and increases for RT4 (21%). It then remains constant for RT5 (21%) and decreases for RT6 (11%) (Figure 5).



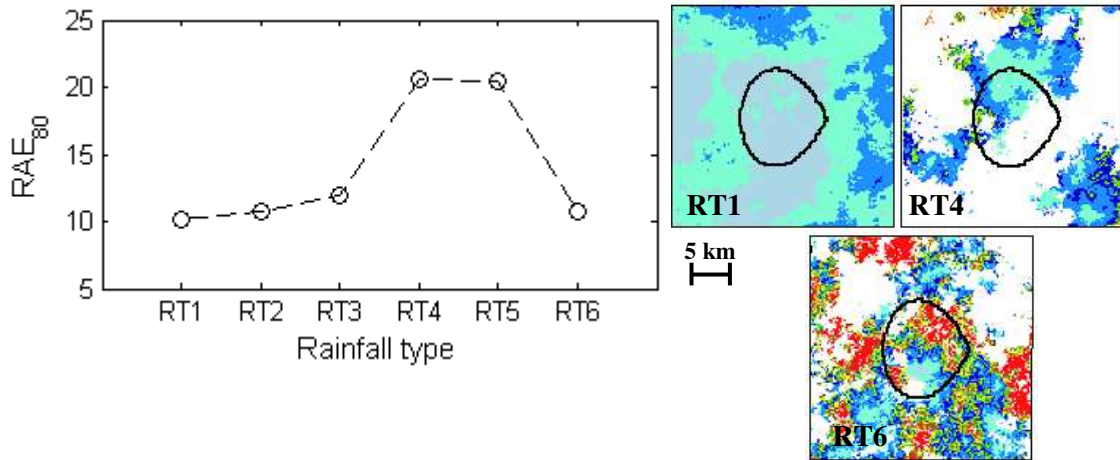


Figure 5: Evolution of  $RAE_{80}$  (in %), computed for the reference scenario, in function of the rainfall type (RT1 to RT6). Rainfall fields have a velocity  $V5$  and an upstream-downstream direction. Example of a simulated image of rainfall field RT1, RT4 and RT6 over the simulation window (the color bar is the same as the one of Figure 2). The  $90 \text{ km}^2$  catchment of intermediate shape is represented.

Those evolutions can be explained in the following way. For the less variable rainfall fields (RT1 and RT2), rainfall is spatially uniform over the catchment (Figure 5). In this case, the differences between distributed and average hydrographs are small. When the spatial variability of rainfall increases (RT4 and RT5), rainfall fields generate contrast over the catchment which results in an increase of  $RAE_{80}$  (an example is given on Figure 5, where it rains only on a part of the catchment). Finally, for the most variable rainfall fields (RT6), the high variability (Figure 5) appears significantly filtered by the catchment and thus an average knowledge of the rainfall spatial variability is not very different from a distributed knowledge.

### Influence of the rainfall direction evaluated on the reference catchment

The influence of rainfall fields' direction is illustrated for the reference catchment scenario with  $V5$ .  $RAE_{80}$  are the highest for the perpendicular direction.  $RAE_{80}$  reaches a value of 28% for RT4 (Figure 6). Moreover,  $RAE_{80}$  is smaller than 12% for a downstream-upstream direction. For the downstream-upstream or upstream-downstream directions, from a time step to another, the rainfall field will pass over different isochrones lines and the spatial variations of rainfall will be filtered by the catchment. For the perpendicular direction, the same rainfall field will stay on the same isochrones line during several time steps. This persistence seems to engender more contrast between a detailed and an average knowledge of rainfall.

We can also notice that the observations made in the previous section concerning the influence of the rainfall type remain verified for the three considered directions.

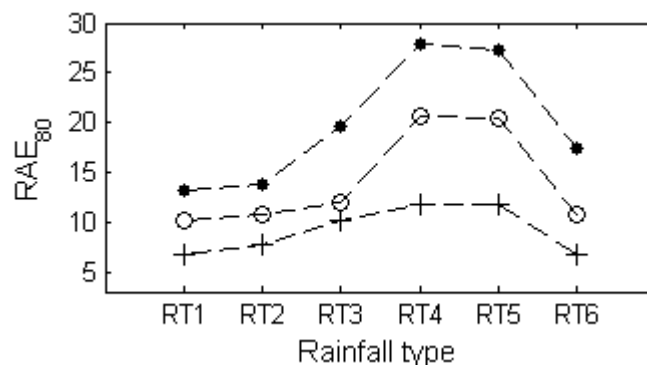


Figure 6: Evolution of  $RAE_{80}$  (in %), for the reference scenario, in function of the rainfall type for the three considered rainfall fields' directions: downstream-upstream (plus), upstream-downstream (circle) and perpendicular (points).

### Influence of the catchment response time – rainfall field velocity

The analysis has been performed for the 90 km<sup>2</sup> catchment, of intermediate shape, with a SCS production function and with different values of ratio of the rainfall field velocity ( $V$ ) by the catchment celerity ( $C$ ) of 2.5, 5 and 10. Those three values of ratio can be obtained for different combinations of values of  $V$  and  $C$ . We have noticed that for the same value of the ratio  $V/C$ , the results are very similar. Thus, those results give rise to a temporal invariant:  $V/C$ . Figure 7 presents the  $RAE_{80}$  evolution for different values of  $V/C$ . The different simulations enable to obtain five values of ratio equal to 1.25, 2.5, 5, 10 and 20. The values of 1.25 and 20 are obtained only with one combination of  $V$  and  $C$ .

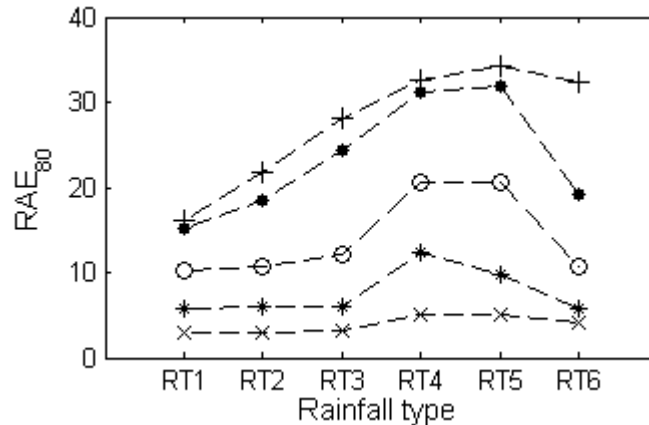


Figure 7: Evolution of  $RAE_{80}$  (in %), for the 90 km<sup>2</sup> catchment with an intermediate shape and a SCS production function, for a ratio  $V/C$  equals to 1.25 (plus), 2.5 (points), 5 (circles), 10 (stars) and 20 (crosses). The rainfall fields' direction is upstream-downstream.

Whatever the rainfall type, the lowest is the ratio  $V/C$ ; the highest are the differences between the distributed and the average hydrographs. For example, for RT4,  $RAE_{80}$  equals to 33% for a ratio of 1.25 against 5% for a ratio of 20. Moreover, when the ratio is high (equals to 10 and 20);  $RAE_{80}$  remains small whatever the rainfall type (equals at a maximum to 12% for a ratio of 10 and to 5% for a ratio of 20). For a ratio of 20, the rainfall type does not have any more influence. This could be explained by the fact that for high values of rainfall field velocity or for small values of catchment celerity, the catchment filters the spatial variations of the successive rainfall fields. Therefore, an average knowledge of rainfall becomes close to a distributed one.

Those observations are made for rainfall fields with an upstream-downstream direction. However, they remain valid whatever the rainfall field direction. The only difference is that, as observed in the previous part,  $RAE_{80}$  have higher values for a perpendicular direction and smaller values for a downstream-upstream direction.

### Influence of the catchment area

Figure 8 presents the evolution of  $RAE_{80}$  for the four considered scenario A270, A90 (Ref), A30 and A10 with a ratio  $V/C$  equals to 5 ( $V$  equals to 5 m/s and  $C$  to 1 m/s) and with an upstream-downstream rainfall field direction.

Values of  $RAE_{80}$  increase with the catchment area. For example, for RT4,  $RAE_{80}$  equals to 26% for the 270 km<sup>2</sup> catchment against 10% for the 10 km<sup>2</sup> catchment. Thus, for the considered rainfall fields, the biggest is the catchment; the highest are the differences between average and distributed hydrographs. Figure 8 illustrates this aspect through an example. The spatial structure of the rainfall field makes it weakly variable over the catchments of 10 km<sup>2</sup> and 30 km<sup>2</sup>. Some significant spatial contrasts appear over the 90 km<sup>2</sup> catchment and become important for the 270 km<sup>2</sup> catchment, for which the differences between distributed and average hydrographs are the highest. We can note that those tendencies are verified for all combinations of rainfall fields' directions and values of  $V/C$ , with however different values of  $RAE_{80}$ .

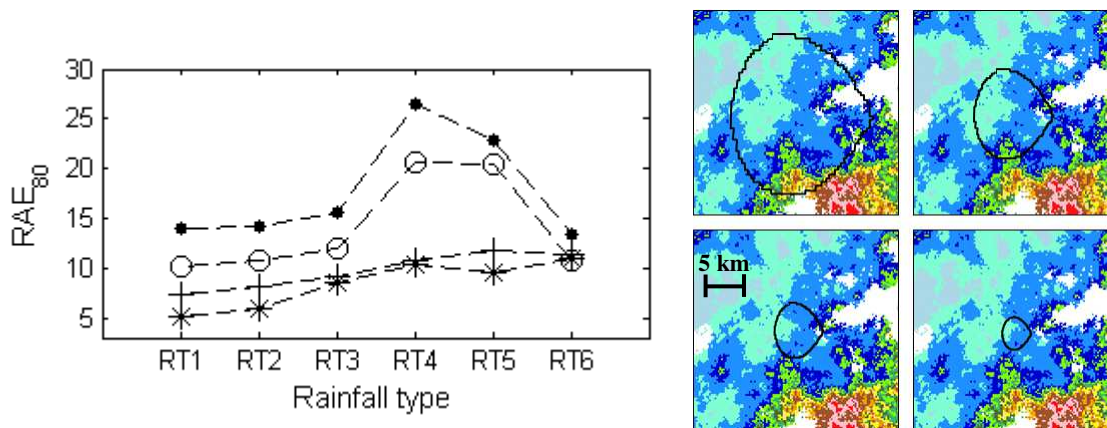


Figure 8: Evolution of  $RAE_{80}$  (in %) in function of the rainfall type for the scenarios: A270 (points), Ref (circles), A30 (plus) and A10 (stars) with V5 and an upstream-downstream direction. Catchments of 270 km<sup>2</sup>, 90 km<sup>2</sup>, 30 km<sup>2</sup> and 10 km<sup>2</sup> are represented over a RT2 rainfall field image.

## CONCLUSION

The objective of this paper has been to quantify the effects of neglecting rainfall spatial variability on the hydrological modelling of catchments of about ten to several hundred km<sup>2</sup>. A simulation approach has been undertaken. The choice has been made not to be exhaustive but to study contrasted situations. Therefore, different configurations of rainfall fields have been considered by simulating time series of rainfall fields with different spatial extents, different velocities and different directions. Those time series of rainfall fields have been associated with different scenarios of catchments, each scenario having a catchment with determined area, shape and hydrological behavior. It appeared that the effects of neglecting rainfall variability were particularly important if: 1) the dimensionless ratio “velocity of rainfall field on celerity along flow path” is small, 2) the rainfall field direction is perpendicular to the catchment flow direction and also if 3) the catchment presents an elongated shape and 4) a Horton or SCS production function. Both last results are not presented in this paper. Results also showed that it is difficult to obtain general conclusions by studying only a few events which contribute to explain the different conclusions reached in the literature.

At last, in order to verify that simulation results are close to reality, all results will have to be confronted to those obtained on real catchments with some real rainfall measurements.

## REFERENCES

- Adams, R., Western, A.W. & Seed, A.W. (2012) An analysis of the impact of the spatial variability in rainfall on runoff and sediment predictions from a distributed model. *Hydrol. Processes*. **26**, 3263-3280.
- Emmanuel, I. (2011) Evaluation de l'apport de la mesure de pluie par radar météorologique pour la modélisation pluie-débit de petits bassins versants. *PhD Thesis*, ECN, Nantes, France.
- Janey, N. (1992) Modélisation et synthèse d'images d'arbres et de bassins fluviaux associant méthodes combinatoire et plongement automatique d'arbres et cartes planaires. *PhD Thesis*, LIFC, Besançon, France.
- Leblois, E. & Creutin, J.-D. (2013) Space-time simulation of intermittent rainfall with prescribed advection field: Adaptation of the turning band method. *Water Resour. Res.* **49**, 3375-3387.
- Moussa, R. (1996) Analytical Hayami solution for the diffusive wave flood routing problem with lateral inflow. *Hydrol. Processes*. **10**, 1209-1227.
- Moussa, R. & Bocquillon, C. (1996) Criteria for the choice of flood-routing methods in natural channels. *J. Hydrol.* **186**, 1-30.
- Quintero, F., Sempere-Torres, D., Berenguer, M. & Baltas, E. (2012) A scenario-incorporating analysis of the propagation of uncertainty to flash flood simulations. *J. Hydrol.* **460-461**, 90-102.
- Schumm, S.A. (1956) Evolution of drainage systems and slopes in badlands at Perth Amboy, New Jersey. *Bul. Geol. Soc. Am.* **67**, 597-646.
- Tarolli, M., Borga, M., Zoccatelli, D., Bernhofer, C., Jatho, N. & Janabi, F. (2013) Rainfall space-time organization and orographic control on flash flood response: the Weissertitz event of August 13, 2002. *J. Hydrol. Eng.* **18**(2), 183-193.
- Zoccatelli, D., Borga, M., Zanon, F., Antonescu, B. & Stancalie, G. (2010) Which rainfall spatial information for flash flood response modelling? A numerical investigation based on data from the Carpathian range, Romania. *J. Hydrol.* **394**(1-2), 148-161.